



ORIGINAL ARTICLE

Dimensional stability and mechanical performance of cement -mortar mix with phragmites-australis fibers at elevated temperature

Rawan Ramadan^a, Jamal Khatib^{a,b}, Elhem Ghorbel^c, Adel Elkordi^{a,d}, Firas Barraj^{e*}, Hassan Ghanem^a

^a Department of Civil Engineering, Beirut Arab University, P.O. Box 11 - 50 - 20 Riad El Solh 11072809, Beirut, Lebanon

^b Faculty of Science and Engineering, University of Wolverhampton, Wolverhampton, WV1 1LY

^c University of Cergy Pontoise, 5 Mail Gay Lussac, Neuville, Oise, 95031, France

^d Department of Civil and Environmental Engineering, Faculty of Engineering, Alexandria University, Alexandria 11 21511, Egypt

^e Faculty of Engineering, University of Balamand, P.O. Box 100, Al Koura 1304, Lebanon

*Corresponding Author: Firas Barraj. Email: f.barraj@balamand.edu.lb

Abstract: The building structure faces the dual challenge of CO₂ emission reduction and performance/sustainability improvement of construction materials. In this respect, in recent times, interest in the incorporation of natural fibers into cementitious systems has been rising as a promising route for attaining these objectives. This paper investigates the effects of adding Phragmites-Australis (Ph-A) fibers on the properties of flexural and compressive strength and length change, including chemical shrinkage, drying shrinkage, and expansion, of cement mortar when exposed to elevated temperature (45 °C). Ph-A fibers were added by volume of mix with different percentages of 0, 0.5, 1 and 2%. Furthermore, a maturity equation was used for the prediction of shrinkage behavior including ultimate shrinkage, time scale factors, and hydration rates. Experimental results revealed that the addition of 1% Ph-A fibers significantly improved flexural and compressive strength while density decreased with increasing fiber content. Besides, the addition of 2% Ph-A fibers reduced chemical shrinkage by 25%, autogenous shrinkage by 12.4%, drying shrinkage by 17.8%, and expansion by 14.9% compared to the control mix. The maturity equation presented very good agreement with the experimental data, confirming its reliability in shrinkage predictions. These results put into evidence the potential of Ph-A fibers to enhance the mechanical and dimensional performance of cement mortar, offering a sustainable solution for reducing environmental impact and advancing durable construction materials.

Keywords: mortar, Ph-A fiber, length stability, mechanical properties, elevated temperature, sustainability

1 Introduction

The construction industry had emerged as one of the most substantial sectors, contributing to approximately 23% of the total carbon dioxide (CO₂) emissions generated by global economic activities

000097-1



Received: 31 March 2025; Received in revised form: 7 August 2025; Accepted: 29 August 2025
This work is licensed under a Creative Commons Attribution 4.0 International License.

[1]. Recognizing its environmental impact, numerous initiatives have been undertaken to foster the development and adoption of sustainable low-carbon building materials [2]. Concrete, being the predominant building material, demands significant energy consumption and extensive use of raw materials during its production. Consequently, efforts have been directed towards exploring various materials to enhance the overall environmental sustainability of concrete such as natural fibers. These fibers have appeared as an effective solution in this attempt due to their perceived sustainability and natural origin [3]. Specifically, plant-based natural fibers have garnered attention as sustainable alternatives to synthetic and steel fibers, owing to their cost-effectiveness, widespread availability, biodegradability, renewability, and low energy requirements [4–10]. Moreover, natural fibers exhibit comparable geometric structures, tensile strength, and Young's modulus compared to synthetic or steel fibers, making them suitable replacements. Research has explored the application of natural fiber-reinforced cement composites in construction materials [11–13]. For example, [14] conducted a study on abaca fiber-reinforced concrete, varying abaca fiber content and length and employing the dry mixing method. Their findings indicated enhanced mechanical performance attributed to fiber reinforcement. Besides, a new plant named *Phragmites-Australis* (Ph-A) has recently been discovered in cementitious system applications. In 2022, [15] revealed that the addition of 1.5% Ph-A enhanced the capillary and total water absorption. In 2024, several studies showed the effect of this plant used as fibers on the volume stability of cement paste and mortar [16–20]. For example, [19] investigated the use of Ph-A plant in cement paste. Results showed that the addition of up to 2% Ph-A reduced the shrinkage of cement and the addition of 1% enhanced the mechanical properties as well.

In another hand, natural fibers consist of chemical components such as cellulose, hemicellulose, lignin, and pectin. When they are incorporated into cementitious materials, these components hinder the initial hydration reaction of cement. Cellulose, a polysaccharide composed of glucose units, undergoes chemical reactions in an alkaline environment [21–24]. These reactions generate acids that neutralize hydroxyl ions produced during cement hydration, resulting in the formation of salts. The accumulation of salts on the clinker surface and hydration products delays the hydration reaction [22, 23]. For example, [24] studied the mechanical properties of hemp fiber-reinforced cement composites. Results show that the alkaline and calcium-rich solutions chemically attacked the fiber surface, decomposing the hemicellulose and causing surface roughening, thereby delaying hydration. In addition to that, [25] demonstrated that the sugar component of wood fibers, like bamboo and oil palm, delayed cement hydration, which was mitigated by using chemical accelerators. Natural fibers generally exhibit high hygroscopicity and possess a bundle-type tubular structure. Consequently, researchers explored the utilization of natural fibers as internal curing agents to mitigate the shrinkage of high-performance cement composites [26–29]. Internal curing technology aims to minimize the risk of cracking in such composites. Some studies [29–31] indicated that saturated natural fibers could serve as internal curing agents in cementitious system. For example, [32] observed that natural fibers possess pores that act as internal curing agents, absorbing and retaining moisture during mixing and releasing it gradually to the cement matrix.

Recently, numerous studies examined the effect of Ph-A fibers on the mechanical properties and volume stability of mortar under standard conditions. However, critical questions remain unanswered regarding the behavior of these fibers under elevated temperatures (45 °C). With growing demand for environmentally friendly building materials, natural fibers like *Phragmites australis* (Ph-A) are being targeted for use in cementitious composites. Sustainability over long-term durability of these materials, especially at elevated temperature, is of particular interest for structural applications. Fiber-reinforced composites may be weakened by fire, hot industrial environments, or thermal cycling. Therefore, determination of the mechanical response of Ph-A fibers at elevated temperatures is important to establish their usability for structural engineering purposes where thermal exposure is anticipated.

Despite the growing body of research, no significant effort has been made to investigate how these fibers impact the volume stability and mechanical properties of mortar in such conditions. This gap in knowledge forms the structure of this study, which employs a series of experimental tests to discover the potential of Ph-A fibers under elevated temperatures.

2 Experimental program

2.1 Materials

In this experiment, Portland cement (PC), siliceous sand and Ph-A fibers were used to create cement-mortar samples. The PC had a density of 1440 kg/m^3 , specific gravity of 3.15 and a fineness of $399.8 \text{ m}^2/\text{kg}$. The siliceous sand had a fineness modulus of 2.8 and a maximum grain size of 2.3 mm. Besides, Ph-A plants, which can grow over 4 meters in height were collected from Bekaa-Lebanon and were selected for their low density of 0.665 g/cm^3 and their ultimate load capacity (27kN). The dry Ph-A stems were cut to a length of 10 mm and wide of 2 mm, treated for 24 h with 4% sodium hydroxide chemical (NaOH) solution and used as fiber addition. Ph-A fiber process is shown in **Fig. 1**.



Fig. 1. Ph-A fiber process

2.2 Mixing proportions

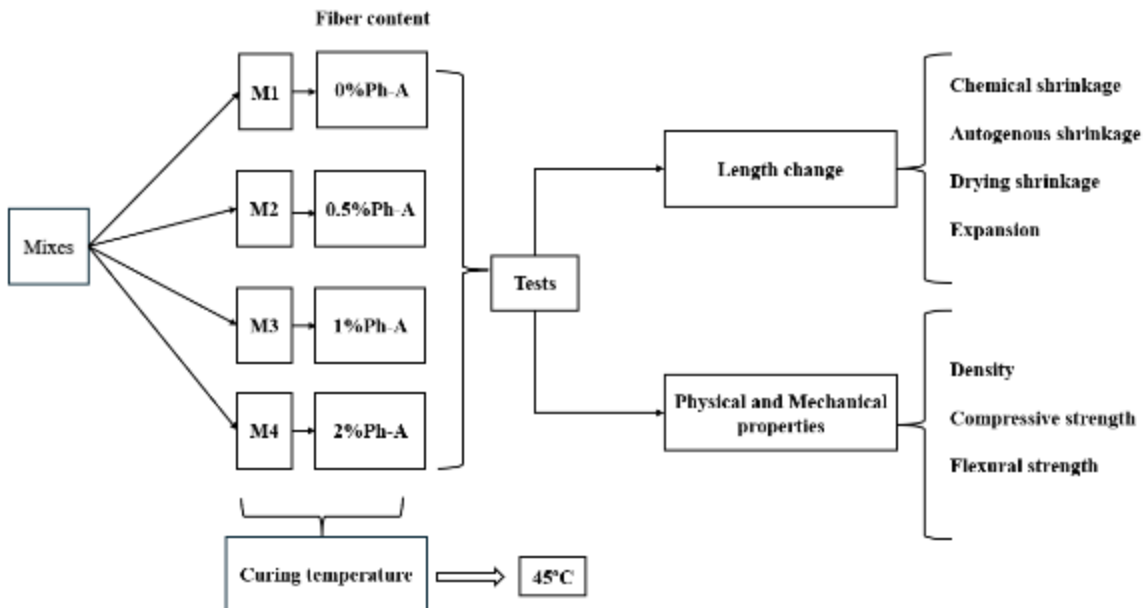


Fig. 2. Graphical presentation of the experimental and testing method

Fiber-reinforced mortars were produced using Ph-A fibers. Mix proportions details are displayed in Tab. 1. Two replicates were made for each type. The water-cement ratio (W/C) and sand-cement ratio (S/C) remained constant at 0.55 and 2 for all mixes, respectively. Ph-A fiber content ranged from 0 to 2% by volume of mortar mix. To ensure that Ph-A fibers were saturated, they were pre-soaked in water for nearly a day and separated from the water just before mixing. A graphical presentation for the experiment and testing method is shown in **Fig. 2**.

Cement and sand were then placed in a mixer and mixed for approximately 25-30 seconds. Subsequently, the distilled water was added and mixed for 1-2 minutes. To ensure proper dispersion of fibers, half of the fiber content was added and mixed for 15 seconds, followed by the addition of the remaining half and thorough mixing at 3-4 minutes. After mixing, the mixture was poured into molds with different dimensions.

Table 1. Table of mixes

Mix nb	Code	Cement	Sand	Ph-A fiber	Water
1	0% Ph-A	617	1233	0	339
2	0.5% Ph-A	617	1233	3.3	339
3	1% Ph-A	617	1233	6.7	399
4	2% Ph-A	617	1233	13.3	399

2.3 Test Methods

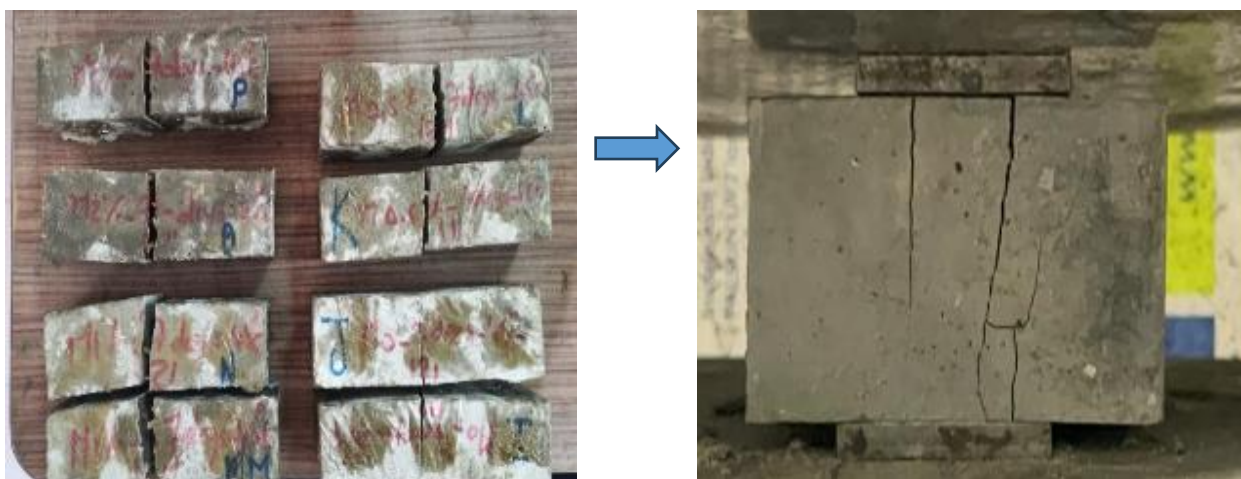


Fig. 3. Flexural and compressive strength test.



Fig. 4. Specimens at 45° C.

For the above mixes mentioned in Tab.1, a total volume of 0.004 m^3 / mix of mortar was prepared to conduct two sets of tests. Firstly, the mechanical tests include compressive and flexural strength, as well as volume stability tests including chemical, drying, autogenous shrinkage and expansion. For flexural strength, two mortar prisms measuring $40 \times 40 \times 160 \text{ mm}^3$ were fabricated at ages of 1, 3, 7, 28, 90 and 180 days for each mix. These mortar specimens underwent curing in an elevated temperature at $45 \pm 2 \text{ °C}$ for 24 hours before being demolded. Subsequently, the demolded specimens were soaked in a container

water bath also maintained at 45 ± 2 °C for water curing. Each mortar specimen was then split into two using the flexural test method, and the compressive strength was measured for each split specimen (as shown in **Fig. 3**). Four split specimens were tested for each mix, and the average value was considered as the result for each age. The flexural and compressive strength tests were conducted following the European standard (EN 1015-11) [33]. It should be noted that before applying flexural strength test, the density test was conducted in accordance with ASTM C138 [34]. Regarding volume stability tests, the chemical shrinkage was performed in accordance with ASTM C1608 [35]. However, drying, autogenous shrinkage as well as expansion were conducted with respect to ASTM C409 [36] Standard. Volume stability tests were also maintained in elevated temperature with three different scenarios: 1-drying shrinkage samples were demolded and exposed directly to an elevated temperature of 45 °C. For autogenous shrinkage, the demolded samples were placed in plastic bags and tightly sealed before being exposed to the same elevated temperature. Regarding expansion, the demolded samples were soaked in water at same elevated temperature conditions. All specimens are shown in **Fig. 4**.

2.4 Predicted -Based Model to assess shrinkage/expansion in mortar

2.4.1 Theoretical maturity model background

The proposed maturity model is initiated in system identification theory, particularly the parameter estimation methodology outlined by [37]. This approach allows the modeling of complex dynamic systems by identifying unknown parameters from input–output data. In the context of cementitious materials, this method was applied to capture the effects of temperature and curing time on hydration and mechanical property development, thereby enabling a more accurate prediction of maturity and performance.

In this paper, authors proposed an empirical model based on maturity concepts to include the natural fibers effect in the prediction of the chemical shrinkage, autogenous shrinkage, drying shrinkage as well as expansion. The determination of the rate of shrinkage and expansion was problematic due to the use of linear regression to fit nonlinear experimental data. The ultimate shrinkage/expansion, the theoretical initial time of shrinkage/expansion, and the rate constant are all important parameters to be determined. For a better nonlinearity account, these parameters are covered within a kinetic model Eq.1 [37, 38].

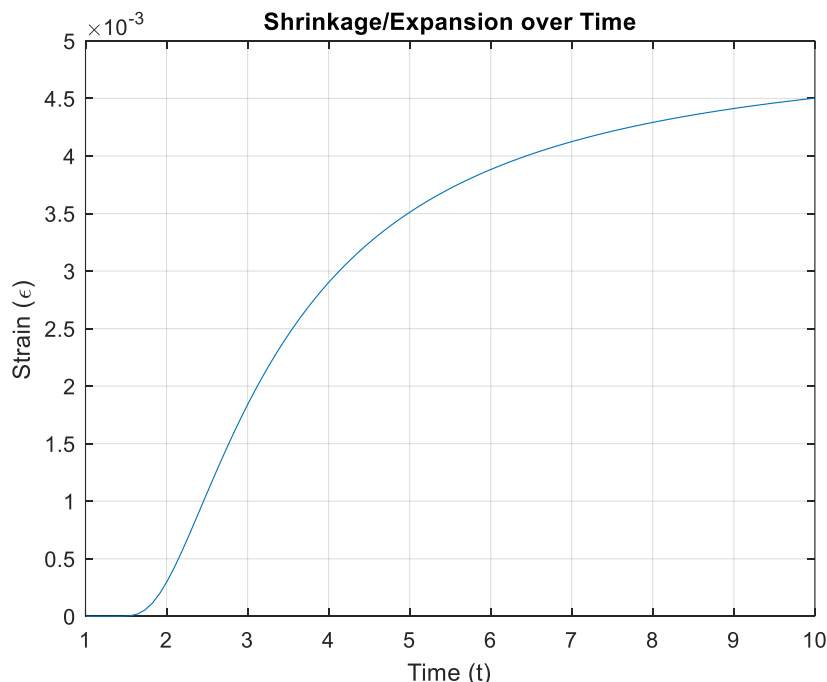


Fig. 5. Maturity model curve.

$$\frac{\varepsilon}{\varepsilon_0} = e^{-\left(\frac{\rho}{t-t_0}\right)^\beta} \quad (1)$$

where ε_0 = ultimate shrinkage/ expansion; β =rate constant; t_0 =initial time of shrinkage / expansion; ρ = time scale factor.

The parameters of the proposed model are determined using a mathematical procedure called system identification SID method [37, 38]. This equation was typed by using Matlab software as follows:

$$\text{epsilon} = \text{epsilon}0 * \exp(-\text{rho} ./ (t - t0)).^\text{beta} ; \quad (2)$$

Fig. 5 presents an example of maturity model curve.

3. Results and Discussions

3.1 Length Change

3.1.1 Chemical Shrinkage

Fig. 6 shows the chemical shrinkage test results under the experimental conditions conducted at 45 °C, highlighting the effects of Ph-A fiber additions in mortar mixes. The proposed maturity equation fits the experimental data very well, reflecting a high degree of reliability of the model. The results indicate that chemical shrinkage decreases with increased content of Ph-A fibers. It presents the highest reduction of about 25% at an addition of 2% Ph-A fiber. Such a reduction in chemical shrinkage may be attributed to the influence of Ph-A fibers on hydration kinetics at an elevated temperature of 45 °C, probably by accelerating the reactions and reducing capillary stresses responsible for shrinkage [17, 39, 40]. Besides, the parameters obtained from the maturity equation further explain this behavior (Tab. 2). At 0% Ph-A, the ultimate chemical shrinkage ε_0 is -734 μE , which at 2% Ph-A is reduced to -540.8 μE , showing that Ph-A fibers were effective in reducing shrinkage. In the same way, the time scale factor from the maturity equation reflects how hydration kinetics change over time under different conditions.

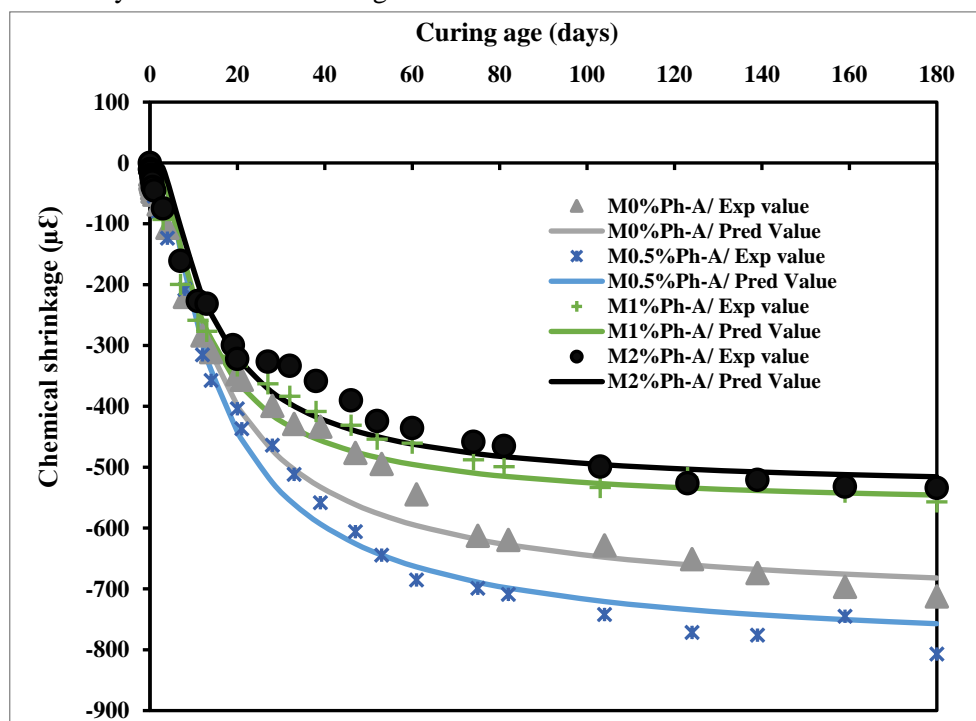


Fig. 6. Chemical shrinkage of mortars with Ph-A fibers at 45 °C.

For chemical shrinkage case, ρ for control mortar mix was 11.98, which was increased to 12.13 for 0.5% Ph-A, indicating a slight acceleration in hydration. Such an increase suggests that low Ph-A content can provide additional nucleation sites, accelerating hydration and inducing more chemical shrinkage. However, for 1% and 2% Ph-A, (ρ) decreased to 9.68 and 11.02, respectively. This reduction indicates that higher Ph-A content disrupts the cementitious matrix, limiting water availability and slowing hydration [39]. Chemical shrinkage is therefore reduced as Ph-A fibers are physical barriers that alter water distribution and hydration kinetics. As a result, Ph-A fibers have dual role in modifying chemical shrinkage, initially enhancing hydration at low percentage but slowing it down at high dosage. Since there is no big difference in the rate constant β remaining at 1 for 0.5% Ph-A and increasing minimally to 1.09 at 2% Ph-A. This suggests that the fundamental hydration kinetics are not substantially changed. However, the minimal increase in β at increased Ph-A % may be a sign of a minimal acceleration of hydration reactions, possibly due to changes in water distribution within the cement matrix [41].

The effect of Ph-A fibers on chemical shrinkage is primarily physical rather than chemical. At low percentage (0.5 Ph-A), the influence is insignificant, and the process of hydration continues as for the control. But at higher Ph-A fiber content (2%), fibers can absorb and retain more water, leading to localized accumulation of available moisture in the matrix [42]. This could be responsible for the slight increase in β . In addition, the fibers also cause heterogeneity at the microstructure level, which can potentially affect the development and distribution of hydration products [27, 28]. Finally, the coefficients of determination R^2 give evidence of the strength of the model, the highest value being 0.991 at 0.5% Ph-A.

3.1.2 Autogenous shrinkage

Fig. 7 displays the autogenous shrinkage test results for mixtures with different contents of Ph-A fibers at a temperature of 45 °C. As shown, the experimental data is in excellent agreement with the proposed maturity equation, as reflected by the strong fit ($0.961 <R^2> 0.973$). It can be realized from the results that there is a trend for autogenous shrinkage to decrease with an increase in the Ph-A fiber content, and the highest reduction of 12.4% was obtained at 2% fiber addition. This reduction can be attributed to the fact that fibers act on the pore structure of the material and diminish self-desiccation effects under hydration [43, 44]. For elevated temperatures, such as 45 °C, hydration kinetics are accelerated and often worsens the autogenous shrinkage due to the rapid consumption of water and the pore pressure that develops. However, the incorporation of Ph-A fibers mitigates these effects by enhancing internal curing and distributing stresses more evenly within the matrix [25, 26]. Furthermore, the derived parameters from the maturity equation (Tab. 2) explain this behavior where ultimate autogenous shrinkage (ϵ_0) goes down significantly from -1930 at 0% Ph-A to -1692 at 2% Ph-A.

Besides, the time scale factor (ρ) represents how the addition of Ph-A fibers modifies the hydration processes. It increases from 21.15 at 0% Ph-A to 30.04 at 2% Ph-A. It shows that Ph-A fibers influence autogenous shrinkage primarily through their physical aspects. The Ph-A fibers, especially at 2% level, act as water retainers, absorbing and distributing water within the matrix. This water retention action delays the initiation of shrinkage by slowing down the rate of water uptake during hydration, which is critical in the case of autogenous shrinkage [40, 41]. These fibers also increase the surface area of the mix, providing self-desiccation mechanism. In another hand, Ph-A fibers restrain the migration of hydration products and water as well, which affects autogenous shrinkage over time. Hence, the time scale factor (ρ) becomes amplified, which displays a more even but slow behavior of shrinking. The invariant rate constant means that Ph-A fibers do not alter the fundamental rate of hydration, but they alter the hydration and microstructural development [16, 20].

The rate constant β is how fast the autogenous shrinkage reaction proceeds. It controls the rate at which the autogenous shrinkage is reached with advancing hydration [45]. Higher β would be the rule when a more rapid shrinking reaction is needed, with reduced β would stand for slower shrinkage. Since β is unchanging in this case, this implies that the rate of hydration that leads to autogenous shrinkage is not significantly altered by Ph-A fibers. However, the slight decrement from 2.27 at 0.5% Ph-A to 2.22 at 2%

Ph-A could imply a slight hydration reduction attributed to the increased water retention and physical confinement due to the presence of Ph-A fibers [26-29]. Despite this minor modification, the fundamental rate of hydration and rate of autogenous shrinkage is not significantly affected [40]. Instead, Ph-A fibers affect only the physical aspects such as water distribution and the formation of microstructural networks [17-19].

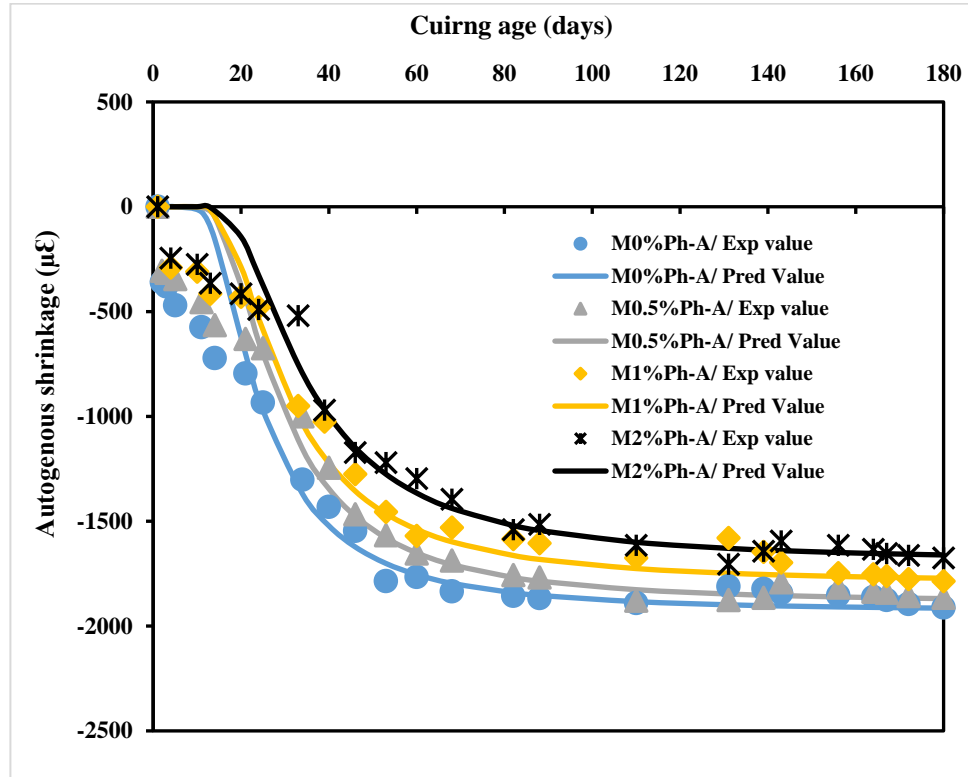


Fig. 7. Autogenous shrinkage of mortars with Ph-A fibers at 45 °C.

3.1.3 Drying shrinkage

Fig. 8 illustrates the results of drying shrinkage performance of mortar mixtures having different percentage replacements of Ph-A fibers, tested under temperature conditions of 45 °C. Like chemical and autogenous shrinkage, the experimental data follows the proposed maturity equation very closely, with R^2 of values between 0.941 and 0.969. There is an explicit trend of drying shrinkage reduction with the rise in the Ph-A fiber content; it can be observed that at 2% fiber content, higher reductions of 17.8% have been obtained compared to the control. This can be explained concerning the ability of the Ph-A fibers in reducing moisture losses and, thus, internal shrinkage stresses [46, 47].

As depicted in Tab. 2, the ultimate drying shrinkage (ε_0) decreases progressively from -2034 for the control mixture (0% Ph-A) to -1693 $\mu\epsilon$ at 2% Ph-A, which means that fibers restrain shrinkage magnitude [18, 19]. The time scale factor (ρ) increases sharply from 18.97 at 0% Ph-A fibers to 35.54 at 2% replacement, which indicates a severe retardation in the initial rate of shrinkage and extended retention of fiber moisture. This increase in ρ signifies the ability of the hydrophilic natural fibers which act as reservoirs to retain moisture in the system and slowing down the evaporation process, which leads to lower drying rates [48]. This is further corroborated by their rough surface texture, which improves bonding interconnection within the matrix. Fibers therefore improve the tortuosity of the system, hindering the diffusion of water and preventing rapid evaporation.

Concurrently, the rate parameter (β), which is the rate of drying shrinkage, shows some scatter. It decreases slightly from 1.6 to 1.55 at 2% Ph-A, suggesting that although the fibers slow the onset of

shrinkage, they reduce the shrinkage rate over time to a little extent. The reduction in β suggests that the fibers would be impacting the hydration environment in such a way that they retard the progression of drying shrinkage and affects their dynamic development [49]. These results confirm that Ph-A fibers are efficient for limiting dry shrinkage when enhanced by elevated temperature [48].

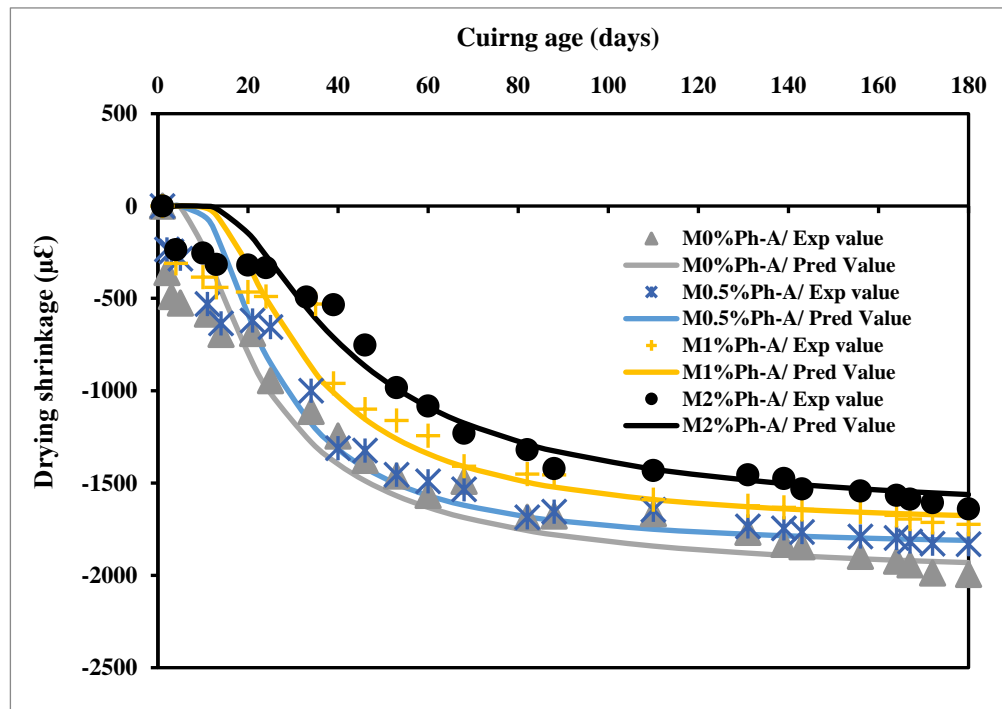


Fig. 8. Drying shrinkage of mortars with Ph-A fibers at 45 °C.

3.1.4. Expansion

Fig. 9 shows the expansion results for mixes with different contents of Ph-A fiber under heat treatment (45 °C). The efficiency of adding Ph-A fibers is reasonably good, just like that of chemical, autogenous, and drying shrinkage. A peak percent decrease of about 14.9% could be observed at a fiber content of 2% from the control mix. Coefficients of determination (R^2) present the proposed maturity equation showing excellent fitness to the experimental results. R^2 ranges from 0.941 to 0.984, further establishing the reliability of the predictive model. This decrease in expansion can be explained by the effect of Ph-A fibers on the thermal response and internal structure of the material [22-25, 49]. Expansion at elevated temperatures is a result of differential stresses due to heat that causes volumetric changes. The fibers have acted as a stabilizing mechanism, hence reducing the intensity of these changes by improving the structural integrity of the matrix and hence limiting thermal gradients [50]. These gradients cause internal stresses that are restrained by the embedded fibers to create observed volumetric expansion—a phenomenon supported by previous studies on thermomechanical and thermal conductivity in heterogeneous cementitious composites [51-53].

The maturity parameters derived agree with these observations (**Tab. 2**). Initial expansion (ε_0) decreases from 2397.572 for the control mixture (0% Ph-A) to 2326.344 at 2% Ph-A, showing the influence of the fibers on expansion retardation. The time scale factor (ρ) evidently increases with fiber content from 10.16 at 0% Ph-A to 29.1 at 2% Ph-A, reflecting a more gradual process of expansion that is substantially delayed [16, 17]. Also, the rate parameter (β) decreases to 0.98 at 2% Ph-A, showing a more gradual course of dilation at higher fiber addition. These results, in addition to the shrinkage data provided above, illustrate the multifunctional role of Ph-A fibers in enhancing the dimensional stability of cement-based materials at elevated temperatures.

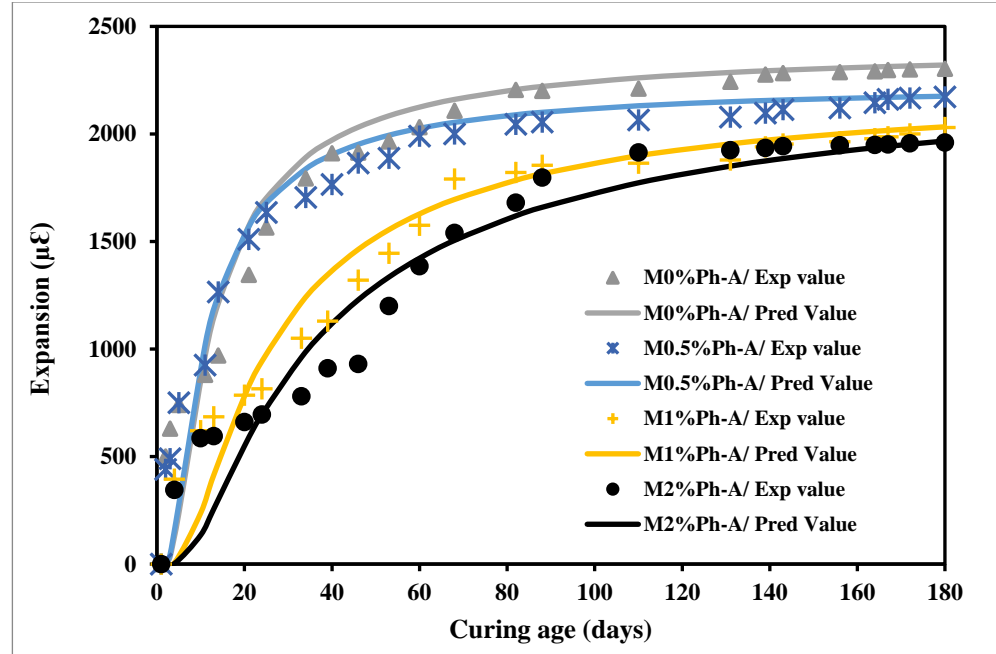


Fig. 9. Expansion of mortars with Ph-A fibers at 45 °C.

Table 2. Maturity equation parameters

Mix Code	Test	\mathcal{E}_0	ρ	β	R^2
0%Ph-A		-734	11.98	0.96	0.979
0.5%Ph-A	Chemical shrinkage	-810	12.13	1	0.991
1%Ph-A		-569.5	9.68	1.08	0.988
2%Ph-A		-540.8	11.02	1.09	0.983
0%Ph-A		-1930	21.15	2.25	0.962
0.5%Ph-A	Autogenous shrinkage	-1890	24.89	2.27	0.97
1%Ph-A		-1795	26.18	2.24	0.972
2%Ph-A		-1692	30.04	2.22	0.969
0%Ph-A		-2034	18.97	1.31	0.943
0.5%Ph-A	Drying shrinkage	-1856	21.69	1.74	0.959
1%Ph-A		-1747	27.37	1.69	0.941
2%Ph-A		-1693	35.54	1.55	0.969
0%Ph-A		2397.57	10.16	1.19	0.984
0.5%Ph-A	Expansion	2229.31	9.04	1.24	0.969
1%Ph-A		2238.11	20.98	1.09	0.957
2%Ph-A		2326.34	29.10	0.98	0.941

To further enhance the proposed maturity model equation, Fig. 10 shows the shrinkage gain for all mixes and for each type of shrinkage. During the initial stages of shrinkage (in the first few days), the gain is fairly weak. For drying, autogenous, and expansion shrinkage, the gain is 17% to 40%, while chemical shrinkage shows a comparably weaker initial gain, from 3% to 40%. This means that the fibers' influence on shrinkage is greater in the later phase than immediately after mixing [16, 18]. The weak initial shrinkage gain could be a result of the fibers' capacity to retain moisture and physically engage with the matrix. During the early age, Ph-A fibers capture and hold water, reducing the rate of evaporation and delivering a gradual rate of hydration [20]. This is why the shrinkage response is delayed, resulting in an early shrinkage rate decrease. But as time elapses, there is a large variation, and the shrinkage gain enhances significantly for all types. At the last stage of 180 days, the shrinkage is around 90-95% of its final value, proving that most of the shrinkage occurs at a longer time interval, and not initially.

The sustained increase in shrinkage can be explained by the sustained activity of fiber-induced water retention, such that slower and incremental movement over time is felt [54, 55]. Although Ph-A fibers restrain early accelerated shrinkage. They do not inhibit shrinkage but retard and delay it. The total shrinkage thus reaches equilibrium at the end of the curing time, showing a more uniform and controlled process of shrinkage. The retarded shrinkage agrees with the observed increment in the time scale factor (ρ) and decrement in the rate parameter (β) for drying, autogenous shrinkage as well as expansion.

The time scale factor increase indicates a delayed onset of shrinkage and increased moisture retention. The minimum reduction in β indicates a slight reduction in the rate of shrinkage with time, which can be attributed to the physical barriers of the Ph-A fibers slowing down the rate at which the moisture is lost from the material [17, 18]. Conversely, chemical shrinkage displays a poorer response to fiber addition, particularly in the initial stages, and is speculated to be due to the comparatively narrower influence of fibers on hydration kinetics [40, 41].

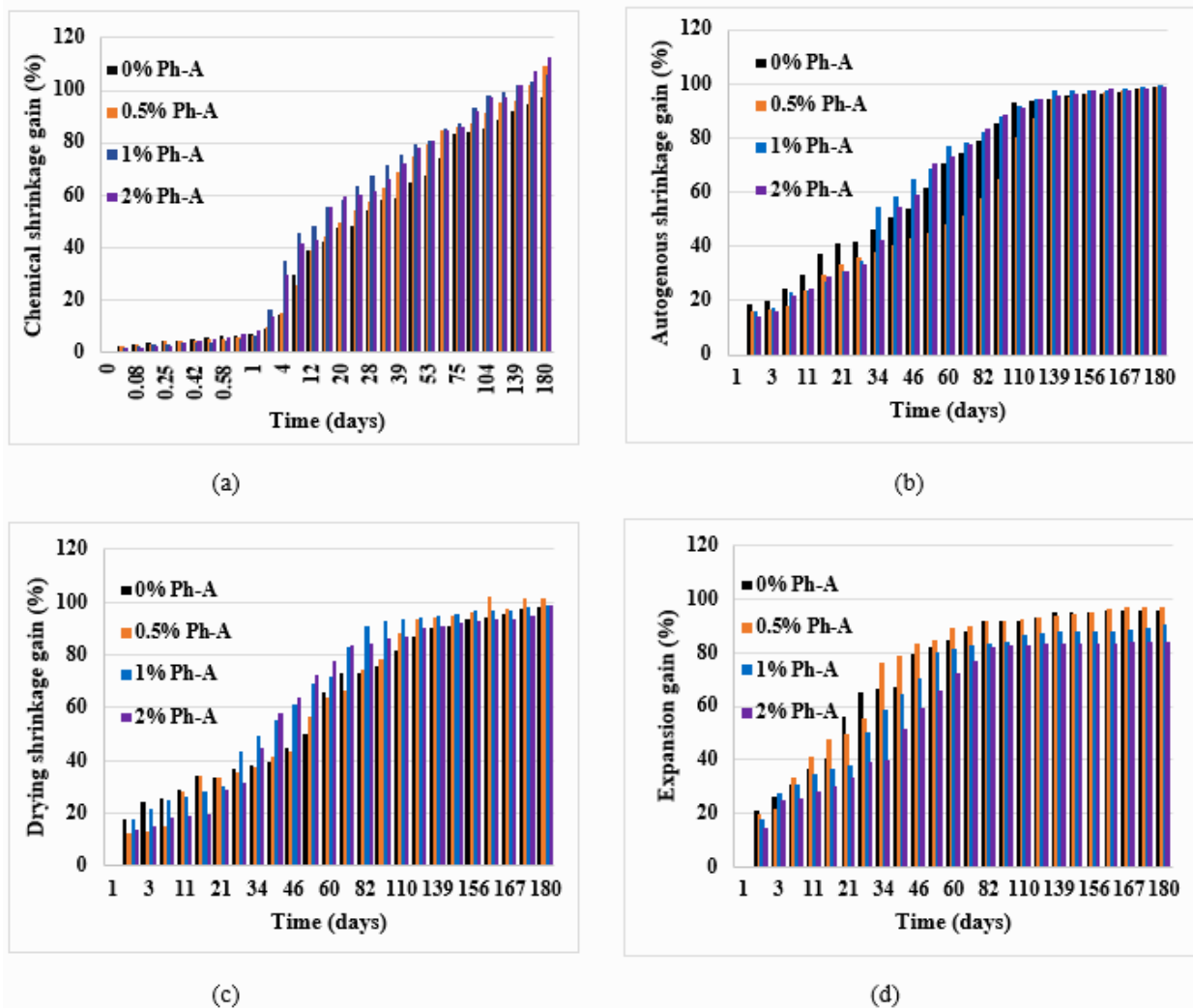


Fig.10. Shrinkage gain for mixes with different percentages of Ph-A fibers at 45 °C.

4.2 Physical and mechanical properties

4.2.1. Density

The density of mortar reinforced with varying percentages of Ph-A fibers is presented in **Fig. 11**. It is

observed that the highest and lowest density is achieved for 0% and 2% Ph-A fibers in all curing ages. For example, at 180 days, a sharp decrease occurs with the inclusion of 2% Ph-A fibers. The value decreases from 2510 to 2370 kg/m³ indicating a decrease of 5.8%. As perceived, the inclusion of Ph-A fibers in mortar results in a decrease in the density. The decrease in density with the addition of 2% Ph-A fibers can be attributed to several physical aspects of the fibers themselves. Natural fibers are lightweight and possess a specific gravity lower than that of cement and sand, and therefore when mixed in, they occupy space without contributing significantly to the mass. Therefore, decreasing the bulk density of the material. In addition, natural fibers are porous and thus may absorb water, leaving small voids in the mixture, increasing the porosity and reducing the packing density [56]. Although direct measurements of porosity were not made for this study, the decrease in density with increasing fiber concentration is likely to reflect an increase in entrapped air or voids when mixing, a phenomenon that has occurred in previous work using Ph-A fibers [57]. This is a working hypothesis with no quantitative measurements of porosity, but follows observations by [17, 18], where fiber addition caused increased internal porosity through the interference with matrix compaction and water retention.

Furthermore, the length and flexibility of the fibers can lead to incomplete mixing and the development of fiber clumps or agglomerates that prevent the effective compaction of the mixture [58]. This prevents close packing of the particles and creates additional voids. Finally, the absorption of water by the fibers can lead to their swelling, with their volume increasing without a corresponding mass increase, which further reduces the matrix density [59, 60]. Besides, as stated by [61]. The increase in fiber content to 2% leads to the increase in absorption due to the increased number of fibers per unit volume and the filling of matrix pores [62-64]. This contributes to the reduction in density.

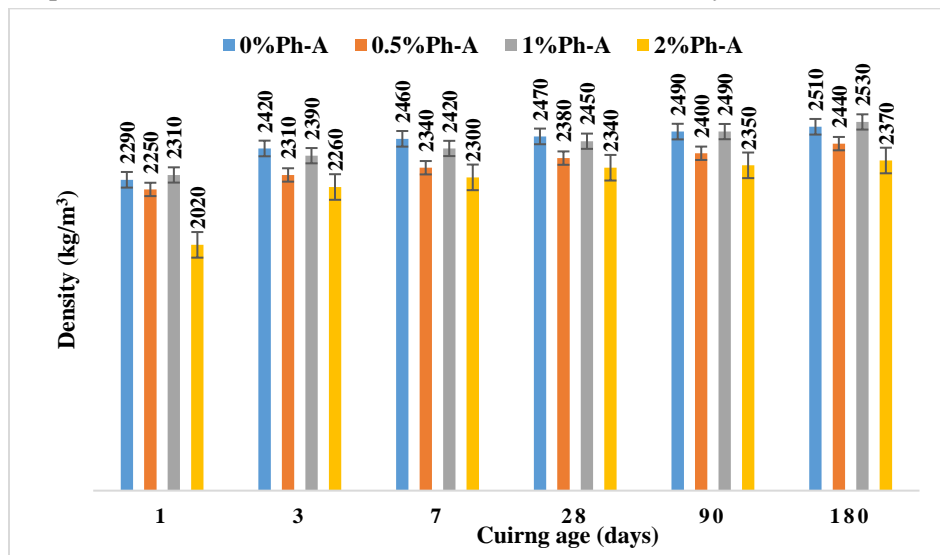


Fig. 11. Density of mortars with Ph-A fibers at 45 °C.

4.2.2. Compressive strength

Fig. 12 focuses on assessing the compressive strength of mortar, with varying additions (0, 0.5, 1 and 2%) of Ph-A fibers, over a 180-curing age. As depicted, the compressive strength slightly decreases with the addition of Ph-A fibers up to 2% Ph-A addition at all percentages compared to the control mix. This reduction can be explained by some grounds because of physical characteristics of the fibers. The addition of fibers to the mixture causes a reduction in the material's overall density and compaction, as mentioned earlier, which can hinder the load-carrying capacity of the material and ultimately reduce the compressive strength. Also, the bond between fiber and matrix can be weaker than cement particle bond, and as the content of fibers increases, the fibers may not be capable of contributing to the total load-carrying capacity of the material [63, 64]. Nevertheless, the minimal improvement in 1% Ph-A fiber content compared to

other Ph-A mixes suggests that at this fiber percentage, the fibers may be capable of contributing to the matrix performance. Although, the compressive strength at 1% incorporation was slightly lower than the control, the overall results remained within a narrow range, indicating no significant adverse effect on strength. It yields a strength of 18.14 MPa at 180-day curing age. At 1% Ph-A addition, the fibers would be able to introduce a level of reinforcement into the mixture, help improve the distribution of loads with imposed loads and resisting micro-cracking within the matrix, thus inducing minor improvement in compressive strength.

The improvement might also result from the fibers' capability to help retain water, leading to improved curing conditions and possibly causing improvement in the process of hydration overall within the mixture [18-22]. More than 1%, the additional fiber content will predominate the mixture and have a dilution effect in which the negative impacts of lower density, compaction, and interfacial bonding between the fibers and matrix overcome the positive impacts of the fibers. Thus, whereas 1% fibers exhibit a slight positive effect on compressive strength, higher fiber content (2%) results in reduced strength due to the additive negative effects. Notably, the function of Ph-A fibers extends beyond enhancing compressive strength. These fibers have demonstrated remarkable performance [65]. PA fibers exhibit excellent thermal stability, allowing them to retain their structural integrity even when exposed to high temperatures (e.g. 45 °C) [66].

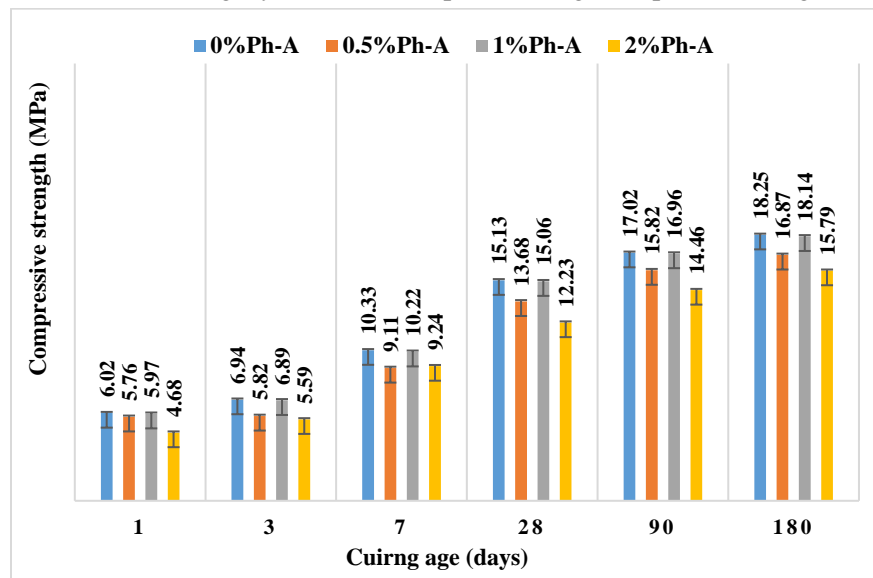


Fig.12. Compressive strength of mortars with Ph-A fibers at 45 °C.

To further illustrate our findings, **Fig. 13** shows the relative compressive strength (RCS) values for control and Ph-A fiber mortar mixes. As observed, there is a clear trend in the variation of strength with fiber content. For 0.5% Ph-A mix, the initial reduction in RCS to a minimum value at 3 days (84%) is attributed to increased porosity and reduced cement particle bonding. However, strength regains steadily with age and is 92% at 180 days, suggesting that the addition of Ph-A fiber does not negatively impact long-term strength. The 1% Ph-A mixture presents a consistent pattern of strength, staying nearly at the control sample level at all curing ages (98–99%), which indicates that 1% Ph-A is an optimal dosage where fiber distribution does not negatively impact cement hydration or cohesion of matrix. Conversely, the highest decrease in RCS is found for the 2% Ph-A addition, particularly at early ages (77% at 1 day, 80% at 3 days), with poor recovery with age (87% at 180 days).

This suggests that excess Ph-A fiber content adversely affects the cement matrix, producing higher void content and weaker bonding, reducing compressive strength [62-65]. Globally, while moderate fiber addition (0.5–1%) produces acceptable strength reductions, higher fiber levels (2%) have significant impacts on compressive performance due to the increased porosity and weaker fiber-matrix interaction [63, 64].

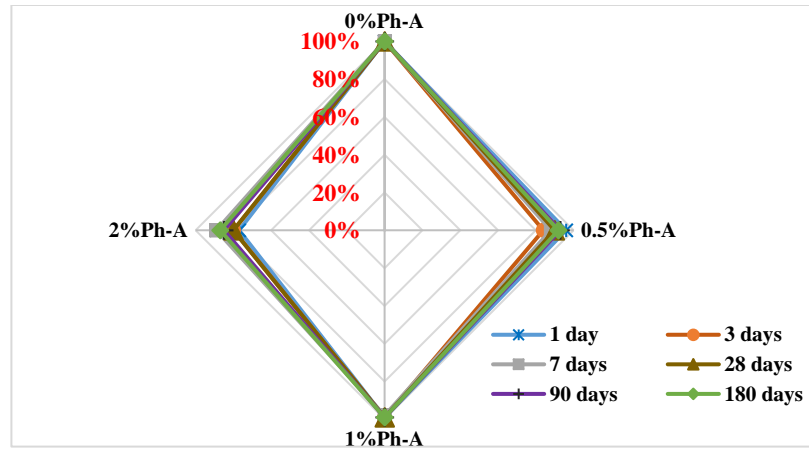


Fig.13. Relative compressive strength for mixes with Ph-A fibers.

4.2.3. Flexural strength

The results for flexural strength of mortars, with varying proportions of Ph-A fibers (0 to 2%) are illustrated in **Fig. 14**. The curing age are 1, 3, 7, 28, 90 and 180 days. As depicted, there is an improvement in flexural strength with the incorporation of Ph-A fibers. The optimal flexural strength is achieved with 1% Ph-A fiber, achieving a value of 9.9 MPa after 180 days, which is equivalent to an increase of 3.98% compared to the control mix. The valuable increased trend in flexural strength up to a 1% threshold can be attributed to the inherent strength of these fibers and their advantageous physical interaction with the matrix [67]. Specially, at elevated temperature (45 °C±1), where the thermal stability of Ph-A would merit further increment [63, 64].

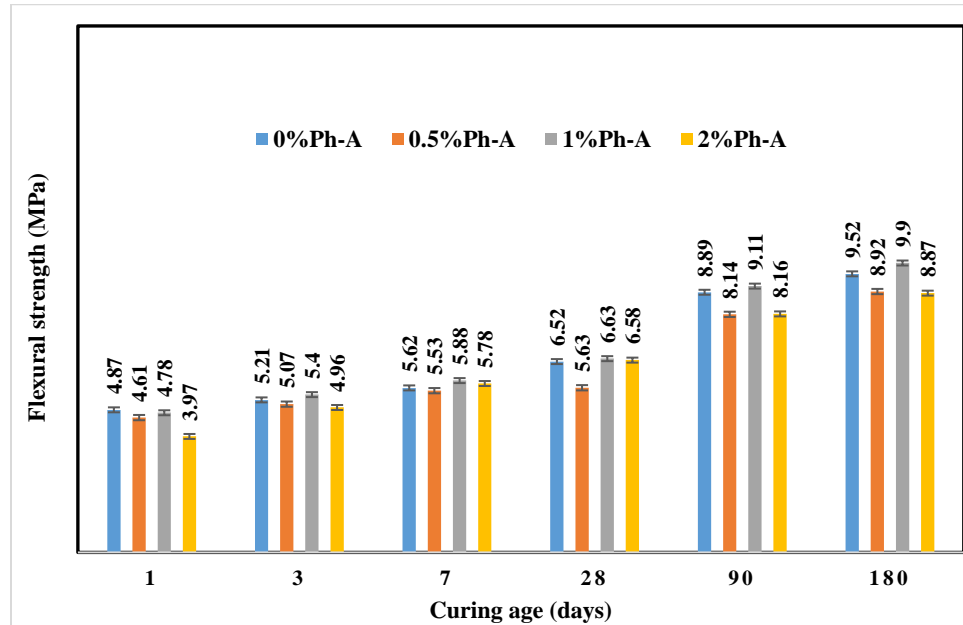


Fig. 14. Flexural strength of mortars with Ph-A fibers at 45 °C.

However, it is noteworthy that beyond this 1% threshold, flexural strength began to decline. This is attributed to several physical property-related factors as well as the interaction between the fibers and matrix. Increasing the fiber content, the fibers were unable to disperse uniformly and instead clumped together with less ability to effectively reinforce the material. This non-uniform distribution creates regions where the fibers cannot efficiently resist bending, and hence the flexural strength reduces [18, 55, 56]. Moreover, the

bond between the fibers and the matrix deteriorates at high fiber content, especially when the fibers are not suitably treated, and induces debonding or pull-out of fibers when subjected to flexural loading [68]. Increased fiber content also results in decreased density and compaction, creating more voids within the matrix, thereby decreasing its overall load-carrying capacity and bending resistance [62]. Also, at higher fiber content, the fibers tend to interfere with the material's load-carrying ability, distorting the integrity of the matrix and resulting in reduced stiffness and flexural strength [69]. Thus, while 1% fibers could record some gain in flexural strength, undesirable in terms of poor distribution, low interfacial bond strength, and reduced density due to more content of fiber aid in bringing the flexural strength down from this level [70, 71]. The fibers have been observed to bridge microcracks and transfer internal tensile stress, thus retarding crack extension when loading. Although no direct stress distribution analysis was performed in this study, similar mechanisms of stress transfer have been observed in natural fiber-reinforced cement composites [72, 73], which attest to this influence at reasonable fiber contents.

5 Conclusions

This paper presents a study on the incorporation of Ph-A fibers in mortar mixes. It revealed the high potential of Ph-A fibers in increasing the mechanical properties and dimensional stability of cement mortar at elevated temperatures. The addition of Ph-A fibers exhibited an increase in strength and a decrease in shrinkage and expansion. The key outcomes of this study are summarized below:

- Density decreases with the increase in Ph-A fiber content. This kind of trend may be interpreted to mean that although fibers enhance mechanical properties, they tend to cause a slight reduction in the weight and density of the mortar; this could reduce the material's durability over a longer period under specific conditions.
- The inclusion of 1% Ph-A fiber showed the most significant improvement in compressive strength compared to other fiber percentages (0.5 and 2%). Besides, for flexural strength, incorporating 1% Ph-A fiber resulted in an increase of 3.98% compared to the control mix, demonstrating its positive effect on the mechanical performance of mortar.
- For shrinkage parameters, the use of 2% Ph-A fibers reduced the chemical shrinkage by 25%, reflecting a reduction in the volume loss during hydration process. Similarly, there has been a reduction in drying, autogenous shrinkage as well as expansion with 2% Ph-A fibers by about 17.8%, 12.4% and 14.9%, which clearly shows improvement in resistance to shrinkage. Fibers seem to decrease the loss of moisture and contribute to the overall reduction of volume change during hydration. Besides, it prevents expansive reactions within cementitious materials and ultimately improves long-term. This indeed improves the dimensional stability of mortars.
- The experimental results are in good agreement with the proposed maturity equation, which showed a very good, best fit. R^2 are between 0.95 and 0.98 for all mixes. These Ph-A fibers appear to influence the material's microstructure and enhance internal curing, hence reducing the negative effects due to moisture loss, while distributing internal stresses more positively. Such changes probably diminish the risk of cracking and deformation that might occur owing to rapid hydration and fluctuation in temperature. Furthermore, the most interesting observation is a significant increase in the time scale factor ρ with the increased content of the Ph-A fibers is indicative that the fibers retard the processes of shrinkage and expansion, turning their character into more smooth and gradual ones. Furthermore, the lessening rate parameter (β) at higher fiber content shows that the fibers help moderate the rate in both shrinkage and expansion.

Further studies are needed to determine the optimal fiber content, long-term durability, and other performance parameters of Ph-A fibers in different environmental conditions.

Acknowledgement

The authors would like to express their sincere gratitude to all those who contributed to the success of this work. Special thanks are extended to the laboratory staff and technical team at Beirut Arab University-

Lebanon for their assistance during the experimental phase.

CRediT authorship contribution statement

Rawan Ramadan: Investigation, Formal analysis, Writing – original draft. **Jamal Khatib and Elhem Ghorbel:** Conceptualization, Funding acquisition, Supervision, Investigation, Formal analysis, Writing – original draft. **Adel Elkordi:** Investigation. **Hassan Ghanem and Firas Barraj:** Supervision, Investigation. **Rawan Ramadan, Firas Barraj:** Supervision, Writing – review & editing.

Conflicts of Interest

The authors declare that they have no conflicts of interest to report regarding the present study.

Data Availability Statement

Some or all data, models, or codes that support the findings of this study are available from the corresponding author upon reasonable request.

References

- [1] Chen J, Shen L, Song X, Shi Q, Li S. An empirical study on the CO₂ emissions in the Chinese construction industry. *Journal of Cleaner production* 2017; 168: 645-654. <https://doi.org/10.1016/j.jclepro.2017.09.072>
- [2] Amziane S, Sonebi M. Overview on biobased building material made with plant aggregate. *RILEM Technical Letters* 2016; (1): 31-38. <https://doi.org/10.21809/rilemtechlett.2016.9>
- [3] Onuaguluchi O, Banthia N. Plant-based natural fibre reinforced cement composites: A review. *Cement and Concrete Composites* 2016; 68: 96-108. <https://doi.org/10.1016/j.cemconcomp.2016.02.014>.
- [4] Pacheco-Torgal F, Jalali S. Cementitious building materials reinforced with vegetable fibres: A review. *Construction and building materials* 2011; 25(2): 575-581. <https://doi.org/10.1016/j.conbuildmat.2010.07.024>
- [5] de Andrade Silva F, Mobasher B, Soranakom C, Toledo Filho R.D. Effect of fiber shape and morphology on interfacial bond and cracking behaviors of sisal fiber cement based composites. *Cement and Concrete Composites* 2011; 33(8): 814-823. <https://doi.org/10.1016/j.cemconcomp.2011.05.003>.
- [6] Toledo Filho R.D, de Andrade Silva F, Fairbairn E.M.R, de Almeida Melo Filho J. Durability of compression molded sisal fiber reinforced mortar laminates. *Construction and building materials* 2009; 23(6): 2409-2420. <https://doi.org/10.1016/j.conbuildmat.2008.10.012>
- [7] Tscheegg E.K, Schneemayer A, Merta I, Rieder K.A. Energy dissipation capacity of fibre reinforced concrete under biaxial tension-compression load. Part I: Test equipment and work of fracture. *Cement and Concrete Composites* 2015; 62: 195-203. <https://doi.org/10.1016/j.cemconcomp.2015.07.002>.
- [8] Tscheegg E.K, Schneemayer A, Merta I, Rieder, K.A. Energy dissipation capacity of fibre reinforced concrete under biaxial tension-compression load. Part II: Determination of the fracture process zone with the acoustic emission technique. *Cement and Concrete Composites* 2015; 62: 187-194. <https://doi.org/10.1016/j.cemconcom.2015.07.003>.
- [9] Acosta-Calderon S, Gordillo-Silva P, García-Troncoso N, Bompa D.V, Flores-Rada J. Comparative evaluation of sisal and polypropylene fiber reinforced concrete properties. *Fibers* 2022; 10(4): 31. <https://doi.org/10.3390/fib10040031>
- [10] Fidelis M.E.A, Toledo Filho R.D, de Andrade Silva F, Mobasher B, Müller S, Mechtcherine V. Interface characteristics of jute fiber systems in a cementitious matrix. *Cement and Concrete Research* 2019; 116: 252-265. <https://doi.org/10.1016/j.cemconres.2018.12.002>.
- [11] Dev B, Rahman A, Alam R, Repon R, Nawab Y. Mapping the progress in natural fiber reinforced composites: preparation, mechanical properties, and applications. *Polymer Composites* 2023; 44(7): 3748-3788. <https://doi.org/10.1002/pc.27376>
- [12] Song H, Liu J, He K, Ahmad W. A comprehensive overview of jute fiber reinforced cementitious composites. *Case Studies in Construction Materials* 2021; 15: e00724. <https://doi.org/10.1016/j.cscm.2021.e00724>
- [13] Awwad E, Mabsout M, Hamad B, Farran M.T, Khatib H. Studies on fiber-reinforced concrete using industrial hemp fibers. *Construction and Building Materials* 2012; 35: 710-717. <https://doi.org/10.1016/j.conbuildmat.2011.09.030>

2.04.119

- [14] Tampi R, Parung H, Djamaruddin R, Amiruddin A.A. Reinforced concrete mixture using abaca fiber. In IOP Conference Series: Earth and Environmental Science 2020; 419(1): 012060. IOP Publishing. DOI. 10.1088/1755-1315/419/1/012060
- [15] Machaka M, Khatib J, Baydoun S, Elkordi A, Assaad J.J. The effect of adding phragmites australis fibers on the properties of concrete. Buildings 2022; 12(3): 278. <https://doi.org/10.3390/buildings12030278>
- [16] Ramadan R, Jahami A, Khatib J, El-Hassan H, Elkordi A. Improving structural performance of reinforced concrete beams with phragmites australis fiber and waste glass additives. Applied Sciences 2023; 13(7): 4206. <https://doi.org/10.3390/app13074206>
- [17] Ramadan R, Khatib J, Ghorbel E, Elkordi A. Effect of adding Phragmites-Australis plant on the chemical shrinkage and mechanical properties of mortar. In International Conference on Bio-Based Building Materials 2023: 573-584. https://doi.org/10.1007/978-3-031-33465-8_43
- [18] Khatib J, Ramadan R, Ghanem H, Elkordi A. Effect of adding Phragmites-Australis Fiber on the mechanical properties and volume stability of mortar. Fibers 2024; 12(2): 14. <https://doi.org/10.3390/fib12020014>
- [19] Ramadan R, Ghanem H, Khatib J.M, ElKordi A.M. Effect of Plant-based natural fibers on the mechanical properties and volume change of cement paste. International Journal of Building Pathology and Adaptation 2024. <https://doi.org/10.1108/IJBPA-11-2023-0166>
- [20] Ghanem H, Ramadan R, Khatib J, Elkordi A. Volume Stability and Mechanical Properties of Cement Paste Containing Natural Fibers from Phragmites-Australis Plant at Elevated Temperature. Buildings 2024; 14(4): 1170. <https://doi.org/10.3390/buildings14041170>
- [21] Li W, Sun B, Wu P. Study on hydrogen bonds of carboxymethyl cellulose sodium film with two-dimensional correlation infrared spectroscopy. Carbohydrate polymers 2009; 78(3): 454-461. <https://doi.org/10.1016/j.carbpol.2009.05.002>
- [22] De La Grée G.D, Yu Q.L, Brouwers H.J.H. Assessing the effect of CaSO₄ content on the hydration kinetics, microstructure and mechanical properties of cements containing sugars. Construction and Building Materials 2017; 143: 48-60. <https://doi.org/10.1016/j.conbuildmat.2017.03.067>
- [23] Pourchez J, Govin A, Grosseau P, Guyonnet R, Guilhot B, Ruot B. Alkaline stability of cellulose ethers and impact of their degradation products on cement hydration. Cement and Concrete Research 2006; 36(7): 1252-1256. <https://doi.org/10.1016/j.cemconres.2006.03.028>
- [24] Sedan D, Pagnoux C, Smith A, Chotard T. Mechanical properties of hemp fibre reinforced cement: Influence of the fibre/matrix interaction. Journal of the European Ceramic Society 2008; 28(1): 183-192. <https://doi.org/10.1016/j.jeurceramsoc.2007.05.019>.
- [25] Sudin, R. and Swamy, N., 2006. Bamboo and wood fibre cement composites for sustainable infrastructure regeneration. Journal of materials science; 41(21): 6917-6924. <https://doi.org/10.1007/s10853-006-0224-3>
- [26] Ramadan R, Elkordi A, Ghorbel E, Ghanem H, Khatib J. Investigating volume stability Performance of paste with Phragmites Australis (PA) Fibers. Procedia Structural Integrity 2024; 64: 1927-1934. <https://doi.org/10.1016/j.prostr.2024.09.261>
- [27] Al-Massri G, Ghanem H, Khatib J, Kırız M.S, Elkordi A. Chemical shrinkage, autogenous shrinkage, drying shrinkage, and expansion stability of interfacial transition zone material using alkali-treated banana fiber for concrete. Journal of Structural Integrity and Maintenance 2024; 9(3): 2390650. <https://doi.org/10.1080/24705314.2024.2390650>
- [28] Al-Massri G, Ghanem H, Khatib J, El-Zahab S, Elkordi A. The Effect of Adding Banana Fibers on the Physical and Mechanical Properties of Mortar for Paving Block Applications. Ceramics 2024; 7(4): 1533-1553. <https://doi.org/10.3390/ceramics7040099>
- [29] Mezencevova A, Garas V, Nanko H, Kurtis K.E. Influence of thermomechanical pulp fiber compositions on internal curing of cementitious materials. Journal of materials in civil engineering 2012; 24(8): 970-975. [https://doi.org/10.1061/\(ASCE\)MT.1943-5533.0000446](https://doi.org/10.1061/(ASCE)MT.1943-5533.0000446)
- [30] Gwon S, Choi Y.C, Shin M. Internal curing of cement composites using kenaf cellulose microfibers. Journal of Building Engineering 2022; 47: 103867. <https://doi.org/10.1016/j.jobe.2021.103867>
- [31] Dávila-Pompermayer R, Lopez-Yepez L.G, Valdez-Tamez P, Juárez C.A, Durán-Herrera A. Lechugilla natural fiber as internal curing agent in self-compacting concrete (SCC): Mechanical properties, shrinkage and durability. Cement and Concrete Composites 2020; 112: 103686. [https://doi.org/10.1016/j.cemconcomp.2020.103686.](https://doi.org/10.1016/j.cemconcomp.2020.103686)
- [32] Jongvisuttisun P, Leisen J, Kurtis K.E. Key mechanisms controlling internal curing performance of natural fibers. Cement and Concrete Research 2018, 107: 206-220., [https://doi.org/10.1016/j.cemconres.2018.02.007.](https://doi.org/10.1016/j.cemconres.2018.02.007)

- [33] EN1015-11. Methods of Test for Mortar for Masonry—Part 11: Determination of Flexural and Compressive Strength of Hardened Mortar. British Standards Institution (BSI) 2007: London, UK.
- [34] ASTM C138/C138M-13; Standard Test Method for Density (Unit Weight), Yield, and Air Content (Gravimetric) of Concrete. American Society for Testing and Materials (ASTM) International: West Conshohocken, PA, USA, 2013: 33
- [35] ASTMC1608. Standard Test Method for Chemical Shrinkage of Hydraulic Cement Paste. American Society for Testing and Materials: West Conshohocken 2007, PA, USA.
- [36] ASTMC490-04. Standard Practice for Use of Apparatus for the Determination of Length Change of Hardened Cement Paste, Mortar, and Concrete. Annual Book of ASTM Standards 2004; 4(4.2): ASTM: Philadelphia 2004, PA, USA.
- [37] Unbehauen H. Introduction to system identification using parameter estimation methods. In Identification of vibrating structures 1982; 53-120. Vienna: Springer Vienna.
- [38] Ghanem H, Zollinger D, Lytton R. Determination of the main parameters of alkali silica reaction using system identification method. *Journal of materials in civil engineering* 2010; 22(9): 865-873. [https://doi.org/10.1061/\(ASCE\)MT.1943-5533.0000086](https://doi.org/10.1061/(ASCE)MT.1943-5533.0000086).
- [39] Ghanem H, Ramadan R, Khatib J, Elkordi A. A review on chemical and autogenous shrinkage of cementitious systems. *Materials* 2024; 17(2): 283. <https://doi.org/10.3390/ma17020283>
- [40] Ghazzawi S, Ghanem H, Khatib J, El Zahab S, Elkordi A. Effect of Olive Waste Ash as a Partial Replacement of Cement on the Volume Stability of Cement Paste. *Infrastructures* 2024; 9(11): 193. <https://doi.org/10.3390/infrastuctures9110193>
- [41] Wang J, Cheng Y, Yuan L, Xu D, Du P, Hou P, Zhou Z, Cheng X, Liu S, Wang Y. Effect of nano-silica on chemical and volume shrinkage of cement-based composites. *Construction and Building Materials* 2020; 247: 118529. <https://doi.org/10.1016/j.conbuildmat.2020.118529>
- [42] Zhang, Z. and Angst, U., 2022. Microstructure and moisture transport in carbonated cement-based materials incorporating cellulose nanofibrils. *Cement and Concrete Research*, 162, p.106990. <https://doi.org/10.1016/j.cemconres.2022.106990>
- [43] Lee G.W, Choi Y.C. Effect of abaca natural fiber on the setting behavior and autogenous shrinkage of cement composite. *Journal of Building Engineering* 2022; 56: 104719. <https://doi.org/10.1016/j.jobe.2022.104719>
- [44] Jaberizadeh M.M, Danoglidis P.A, Shah S.P, Konsta-Gdoutos M.S. Eco-efficient cementitious composites using waste cellulose fibers: Effects on autogenous shrinkage, strength and energy absorption capacity. *Construction and Building Materials* 2023; 408: 133504. <https://doi.org/10.1016/j.conbuildmat.2023.133504>
- [45] Zhang Z, Scherer G.W. Measuring chemical shrinkage of ordinary Portland cement pastes with high water-to-cement ratios by adding cellulose nanofibrils. *Cement and Concrete Composites* 2020; 111: 103625. <https://doi.org/10.1016/j.cemconcomp.2020.103625>
- [46] Concha-Riedel J, Araya-Letelier G, Antico F.C, Reidel U, Glade A. Influence of jute fibers to improve flexural toughness, impact resistance and drying shrinkage cracking in adobe mixes. *Earthen Dwellings and Structures: Current Status in their Adoption 2019*: 269-278. https://doi.org/10.1007/978-981-13-5883-8_24
- [47] Yousefieh N, Joshaghani A, Hajibandeh E, Shekarchi M. Influence of fibers on drying shrinkage in restrained concrete. *Construction and Building Materials* 2017; 148: 833-845. <https://doi.org/10.1016/j.conbuildmat.2017.05.093>
- [48] Hojati M, Rajabipour F, Radlińska A. Drying shrinkage of alkali-activated cements: effect of humidity and curing temperature. *Materials and Structures* 2019; 52: 1-14. <https://doi.org/10.1617/s11527-019-1430-1>
- [49] Aluko O.G, Yatim J.M, Kadir M.A.A, Yahya K. A review of properties of bio-fibrous concrete exposed to elevated temperatures. *Construction and Building Materials* 2020; 260: 119671. <https://doi.org/10.1016/j.conbuildmat.2020.119671>
- [50] Poletto M, Júnior H.L.O, Zattera A.J. Thermal decomposition of natural fibers: kinetics and degradation mechanisms. *Reactions and mechanisms in thermal analysis of advanced materials 2015*: 515-545. <https://doi.org/10.1002/9781119117711.ch21>
- [51] Khaliq W, Kodur V. Thermal and mechanical properties of fiber reinforced high performance self-consolidating concrete at elevated temperatures. *Cement and Concrete Research* 2011; 41(11):1112-1122. <https://doi.org/10.1016/j.cemconres.2011.06.012>
- [52] Bentz D.P, Turpin R. Potential applications of phase change materials in concrete technology. *Cement and Concrete Composites* 2007; 29(7): 527-532. <https://doi.org/10.1016/j.cemconcomp.2007.04.007>
- [53] Ahmed W, Lim C.W, Akbar A. Influence of elevated temperatures on the mechanical performance of sustainable-fiber-reinforced recycled aggregate concrete: a review. *Buildings* 2022; 12(4): 487. <https://doi.org/10.3390/buildings12040487>

ings12040487

[54] Ahamed M.S, Ravichandran P, Krishnaraja A.R., 2021, February. Natural fibers in concrete—A review. In IOP Conference Series: Materials Science and Engineering 2021; 1055(1):012038. IOP Publishing.

[55] Geremew A, De Winne P, Demissie T.A, De Backer H. Treatment of natural fiber for application in concrete pavement. Advances in Civil Engineering 2021; 2021(1): 6667965. <https://doi.org/10.1155/2021/6667965>

[56] Falliano D, De Domenico D, Ricciardi G, Gugliandolo E. Compressive and flexural strength of fiber-reinforced foamed concrete: Effect of fiber content, curing conditions and dry density. Construction and building materials 2019; 198: 479-493. <https://doi.org/10.1016/j.conbuildmat.2018.11.197>

[57] Dallel R, Kesraoui A, Seffen M. Biosorption of cationic dye onto "Phragmites australis" fibers: Characterization and mechanism. Journal of environmental chemical engineering 2018; 6(6): 7247-7256. <https://doi.org/10.1016/j.jece.2018.10.024>

[58] Kankılıç G.B, Metin A.Ü. Phragmites australis as a new cellulose source: extraction, characterization and adsorption of methylene blue. Journal of Molecular Liquids 2020; 312: 113313. <https://doi.org/10.1016/j.molliq.2020.113313>

[59] Ghanem H, El Bouz C, Ramadan R, Trad A, Khatib J, Elkordi A. Effect of Incorporating Cement and Olive Waste Ash on the Mechanical Properties of Rammed Earth Block. Infrastructures 2024; 9(8): 122. <https://doi.org/10.3390/infrastructures9080122>

[60] Al-Ghaban A, Jaber H, Shaher A.A. Investigation of addition different fibers on the performance of cement mortar. Engineering and Technology Journal 2018; 36(9A): 957-965.

[61] Teixeira R.S, Bufalino L, Tonoli G.H.D, dos Santos S.F, Junior H.S. Coir fiber as reinforcement in cement-based materials. In Advances in Bio-Based Fiber 2022: 707-739. Woodhead Publishing.

[62] Ahmad J, Aslam F, Martínez-García R, de Prado-Gil J, Abbas N, Hechmi EI Ouni M. Mechanical performance of concrete reinforced with polypropylene fibers (PPFs). Journal of Engineered Fibers and Fabrics 2021; 16:15589250211060399. <https://doi.org/10.1177/15589250211060399>

[63] Çavdar A. A study on the effects of high temperature on mechanical properties of fiber reinforced cementitious composites. Composites Part B: Engineering 2012; 43(5): 2452-2463

[64] Morsy M.S, Rashad A.M, Shebl S.S. Effect of elevated temperature on compressive strength of blended cement mortar. Build Research Journal 2008; 56(2-3): 173-185.

[65] Serri E, Othuman Mydin M.A, Suleiman M.Z. Thermal properties of Oil Palm Shell lightweight concrete with different mix designs. JurnalTeknologi 2014; 70(1): 155-159. <https://doi.org/10.11113/jt.v70.2507>

[66] Rai A, Joshi Y. P. Applications and Properties of Fibre Reinforced Concrete. Journal of Engineering Research and Applications 2014; 4(5): 123-131.

[67] Bessadok A, Roudesli S, Marais S, Follain N, Lebrun, L. Alfa fibers for unsaturated polyester composites reinforcement: Effects of chemical treatments on mechanical and permeation properties. Composites Part A: Applied Science and Manufacturing 2009; 40(2): 184-195. <https://doi.org/10.1016/j.compositesa.2008.10.018>

[68] Gani A, Ibrahim M, Ulmi F, Farhan, A. The influence of different fiber sizes on the flexural strength of natural fiber-reinforced polymer composites. Results in Materials 2024; 21: 100534. <https://doi.org/10.1016/j.rinma.2024.100534>

[69] Chahar M, Kumar R, Habeeb A, Kumar Garg R, Punia U. Factors affecting flexural and impact strength of natural fiber reinforced polymer composites: A review. Green Materials 2024: 1-16. <https://doi.org/10.1680/jgrma.24.0108>

[70] Zhang, T., Yin, Y., Gong, Y., & Wang, L. (2020). Mechanical properties of jute fiber-reinforced high-strength concrete. Structural Concrete, 21(2), 703-712. <https://doi.org/10.1002/suco.201900012>

[71] Bheel, N., Sohu, S., Awoyera, P., Kumar, A., Abbasi, S.A. and Olalusi, O.B., 2021. Effect of wheat straw ash on fresh and hardened concrete reinforced with jute fiber. Advances in Civil Engineering 2021(1); 6659125. <https://doi.org/10.1155/2021/6659125>

[72] Savastano Jr H, Warden P. G, Coutts R. S. P. Microstructure and mechanical properties of waste fibre-cement composites. Cement and Concrete Composites 2005; 27(5): 583–592. <https://doi.org/10.1016/j.cemconcomp.2004.09.003>

[73] Bentur, Mindess, 2007: Bentur A, Mindess S. Fibre reinforced cementitious composites (2nd ed.). CRC Press 2007; 9780419235306.